Available online at www.sciencedirect.com
SciVerse ScienceDirect
Procedia Engineering 25 (2011) 435 – 438
Procedia Engineering
www.elsevier.com/locate/procedia

Proc. Eurosensors XXV, September 4-7, 2011, Athens, Greece

A Refined Modeling for the Liquid Loading Effect in Microacoustic Sensors

Thomas Voglhuber-Brunnmaier*, Bernhard Jakoby

Johannes Kepler University
Institute for Microelectronics and Microsensors
Altenbergerstr. 69, 4040 Linz, Austria

Abstract

The liquid loading effect on microacoustic sensors can be modeled using an acoustic impedance boundary condition. A rigorous expression for the acoustic impedance tensor is derived for isotropic linear elastic layers backed by a defined impedance. This formulation is generalized to enclose viscous liquids. Furthermore, the impedance tensor is also applied to the half-space, free surface and rigid backing boundary conditions and is compared to the one dimensional expressions of bulk impedance for the half-space and the transmission line equations for layers of finite thickness. In contrast to these 1D expressions, the coupling of pressure- and shear-wave propagation is considered which results in interesting phenomena for viscous liquid layers. For example, it is found that also for liquid layers much thicker than the decay length of the shear waves (e.g., hundreds of nanometers for a QCR in the lower MHz range), the boundary affects the shear impedance, due to pressure and shear wave coupling.

Keywords: Acoustic Impedance Tensor; Wave Coupling; Viscosity; Lame Parameters; Transmission Line Models

1. Introduction

Piezoelectric disc sensors vibrating in thickness shear mode are widely used as fluidic sensors e.g., to measure rheological parameters. For instance, shifts of the resonance frequency induced by the liquid loading can be translated to the mass-density product of the fluid by the Kanazwa and Gordon formula [1]. Such formulas are mostly one dimensional approximations assuming that the resonator faces are infinitely extended in lateral directions and vibrating uniformly. In practice, the area of vibration e.g., of thickness shear sensors is limited and therefore, a non-uniform distribution of the velocity profile results (see Fig 1). Due to this, a certain amount of energy of the dominant shear mode is radiated as pressure waves. The calculation of the characteristic decay length of shear waves suggests that for modeling the usage of a half-space boundary condition (infinitely extended liquid in direction of radiation) is valid

*Corresponding Author: Thomas Voglhuber-Brunnmaier, Phone: +43 732 2468 6267; Fax: +43 732 2468 6252
E-mail address: thomas.voglhuber@jku.at

doi:10.1016/j.proeng.2011.12.108

for shear resonators. However, the damping coefficients of the pressure waves (which are also excited due to non-uniform excitation) are usually small. Hence, for reasonable geometries, reflections at opposing boundaries occur, which are reflected backwards. They affect the apparent acoustic impedance due to pressure to shear wave coupling. For calculations, the equations of motion are partially transformed to the spectral (wavenumbers k_x,k_y) domain by means of a Fourier transform, yielding an ordinary differential equation (ODE). The basic modeling approach is demonstrated in more detail in [2] and has also been used by [3, 4, 5]. Based on the ODE, formulas for the (spectral, i.e., wave number and frequency dependent) acoustic impedance tensor (AIT) are derived. These formulas can be used to calculate interfacial forces induced by arbitrary velocity profiles, efficiently.

2. Modeling

For acoustic wave phenomena in liquids, the linearized Navier-Stokes equations can be applied, which closely resemble the equations for elastic solids. Thus, in the following the theory is first developed for elastic media and generalized later. The equation of motion for a particle in an elastic medium is given by $\rho\ddot{\boldsymbol{u}} = \nabla\cdot(\boldsymbol{c} : \nabla_s\boldsymbol{u})$ where $\boldsymbol{u}$, ρ, $\boldsymbol{c}$, and ∇_s represent displacement vector, mass density, elastic stiffness tensor[a], and the symmetric gradient operator [7]. The equation is partially transformed to the spectral domain by means of a Fourier transform with the correspondences[b] $\{x, y, t\}\circ\!\!-\!\!\bullet\{jk_x, jk_y, j\omega\}$ resulting in a system of ODEs of first order of dimension six (see also [2]):

$$\frac{\partial}{\partial z}\tilde{\boldsymbol{\psi}}(k_x, k_y, z, \omega) = \boldsymbol{A}(\rho, \lambda, \mu, k_x, k_y, \omega)\cdot\tilde{\boldsymbol{\psi}}(k_x, k_y, z, \omega) \ \text{ with } \ \tilde{\boldsymbol{\psi}}(k_x, k_y, z, \omega) = \begin{bmatrix}\tilde{\boldsymbol{v}}(k_x, k_y, z, \omega)\\ \tilde{\boldsymbol{T}}_n(k_x, k_y, z, \omega)\end{bmatrix}. \tag{1}$$

The field variables $\tilde{\boldsymbol{\psi}}$ consist of the velocities $\tilde{\boldsymbol{v}} = [\tilde{v}_x, \tilde{v}_y, \tilde{v}_z]$ and the stress components $\tilde{\boldsymbol{T}}_n = \left[\tilde{T}_{xz}, \tilde{T}_{yz}, \tilde{T}_{zz}\right]^T$ related to the normal direction z. For the calculation of the AIT (components are defined by $Z_{ij} = -T_{n,i}/v_j$) this is an advisable choice. The principal solution of Eq. 1 is given by $\tilde{\boldsymbol{\psi}}(z) = \boldsymbol{X}(z)\cdot\boldsymbol{q}$ with the fundamental system $\boldsymbol{X}(z)$ and the vector of the expansion coefficients[c] $\boldsymbol{q}$. In the following, AITs are calculated for a material layer of thickness d backed by a defined impedance tensor $\tilde{\boldsymbol{Z}}_0$. The fundamental system $\boldsymbol{X}(z)$ in terms of the eigenvector matrix $\boldsymbol{V}$ and the eigenvalues $\pm l_s$ (shear mode), $\pm l_p$ (pressure mode) of $\boldsymbol{A}$ in Eq.1 is given by

$$\boldsymbol{X}(z) = \boldsymbol{V}\cdot\mathrm{diag}[e^{-l_s z}, e^{-l_s z}, e^{-l_p z}, e^{l_s z}, e^{l_s z}, e^{l_p z}] = \begin{bmatrix}\boldsymbol{V}_{11} & \boldsymbol{V}_{12}\\ \boldsymbol{V}_{21} & \boldsymbol{V}_{22}\end{bmatrix}\cdot\begin{bmatrix}\boldsymbol{E}_1(z) & \boldsymbol{0}\\ \boldsymbol{0} & \boldsymbol{E}_2(z)\end{bmatrix} \tag{2}$$
$$\text{with } \boldsymbol{E}_1(z) = \mathrm{diag}[e^{-l_s z}, e^{-l_s z}, e^{-l_p z}] \text{ and } \boldsymbol{E}_2(z) = \mathrm{diag}[e^{l_s z}, e^{l_s z}, e^{l_p z}].$$

The definitions of the submatrices $\boldsymbol{V}_{11}\ldots\boldsymbol{V}_{22}$ and the eigenvalues l_s, l_p are given in appendix A.

2.1. Layer backed by an acoustic impedance tensor $\tilde{\boldsymbol{Z}}_0$

The layer of thickness d is backed by an acoustic impedance tensor $\tilde{\boldsymbol{Z}}_0$ (relating $\tilde{\boldsymbol{T}}_n(d) = -\tilde{\boldsymbol{Z}}_0\cdot\tilde{\boldsymbol{v}}(d)$) yielding the velocity induced stresses

$$\tilde{\boldsymbol{T}}_n(0) = \begin{bmatrix}\boldsymbol{V}_{21} & \boldsymbol{V}_{22}\end{bmatrix}\cdot\boldsymbol{q} \quad \text{with} \quad \boldsymbol{q} = \begin{bmatrix}\boldsymbol{V}_{11} & \boldsymbol{V}_{12}\\ \underbrace{(\tilde{\boldsymbol{Z}}_0\boldsymbol{V}_{11}+\boldsymbol{V}_{21})}_{\boldsymbol{V}_{x1}}\boldsymbol{E}_1(d) & \underbrace{(\tilde{\boldsymbol{Z}}_0\boldsymbol{V}_{12}+\boldsymbol{V}_{22})}_{\boldsymbol{V}_{x2}}\boldsymbol{E}_2(d)\end{bmatrix}^{-1}\cdot\begin{bmatrix}\tilde{\boldsymbol{v}}(0)\\ \boldsymbol{0}\end{bmatrix}. \tag{3}$$

The direct inversion of the matrix in Eq. 3 is numerically critical if the layer is much thicker than the characteristic decay length of shear waves. This is predominantly an issue for liquids (The adaption of the method for liquids is illustrated in section 2.4.) but can also occur in elastic media with high loss moduli (because $\boldsymbol{E}_2(d)$ tends to values which are too large for representation e.g., in MATLAB). The problem is handled by splitting the fundamental system $\boldsymbol{X}$ (see Eq. 2, right hand side) and eliminating the matrix $\boldsymbol{E}_2(d)$. Finally, the general stable formulation for the AIT can be given by:

$$\boxed{\tilde{\boldsymbol{Z}} = \boldsymbol{V}_{21}\left(\boldsymbol{V}_{12}\boldsymbol{E}_1(d)\boldsymbol{V}_{x2}^{-1}\boldsymbol{V}_{x1}\boldsymbol{E}_1(d) - \boldsymbol{V}_{11}\right)^{-1} + \boldsymbol{V}_{22}\boldsymbol{E}_1(d)\left(\boldsymbol{V}_{x2} - \boldsymbol{V}_{x1}\boldsymbol{E}_1(d)\boldsymbol{V}_{11}^{-1}\boldsymbol{V}_{12}\boldsymbol{E}_1(d)\right)^{-1}\boldsymbol{V}_{x1}\boldsymbol{E}_1(d)\boldsymbol{V}_{11}^{-1}}. \tag{4}$$

[a]In our formulation, $\boldsymbol{c}$ consists of the Lamé parameters λ and μ (a.k.a. shear modulus), which are best suited to represent isotropic media. They are related to Young's modulus Y and Poisson's ratio ν by $\lambda = \frac{\nu Y}{(1+\nu)(1-2\nu)}$ and $\mu = \frac{Y}{2(1+\nu)}$ [6].

[b]In the remainder of the paper quantities associated with the spectral domain are denoted by a tilde.

[c]Constant arguments are repressed for clarity.

2.2. *Rigid backing, free surface and semi-infinite medium*

The general formulation in Eq. 4 is evaluated for the special cases of a semi-infinite layer, rigid backing, and free surface. To account for a rigid backing of the material layer of thickness d (i.e., $\tilde{\boldsymbol{v}}(d) = \boldsymbol{0}$) set $\boldsymbol{V}_{x1} = \boldsymbol{V}_{11}$ and $\boldsymbol{V}_{x2} = \boldsymbol{V}_{12}$. If the layer has a free surface at $z = d$ (i.e., $\tilde{\boldsymbol{T}}_n(d) = \boldsymbol{0}$) then set $\boldsymbol{V}_{x1} = \boldsymbol{V}_{21}$ and $\boldsymbol{V}_{x2} = \boldsymbol{V}_{22}$. For a semi-infinite layer set $\boldsymbol{V}_{x1} = \boldsymbol{0}$ which reduces Eq. 4 to $\tilde{\boldsymbol{Z}} = -\boldsymbol{V}_{21}\boldsymbol{V}_{11}^{-1}$.

2.3. *Acoustic impedance tensor for plane wave excitation*

For plane waves ($k_x = k_y = 0$) the fields in x, y, z are not coupled and the AIT (and also $\boldsymbol{V}_{11} \dots \boldsymbol{V}_{22}$) becomes diagonal, containing the expressions known from one dimensional calculations. The impedance of the semi-infinite medium reduces to the specific bulk impedances $\tilde{\boldsymbol{Z}} = \mathrm{diag}\left[Z_s, Z_s, Z_p\right] = \mathrm{diag}\left[\sqrt{\rho\mu}, \sqrt{\rho\mu}, \sqrt{\rho(2\mu+\lambda)}\right]$. The AIT of a layer backed by $\tilde{\boldsymbol{Z}}_0$ reduces to the acoustic transmission line expressions:

$$\tilde{\boldsymbol{Z}} = \mathrm{diag}\left[Z_s\frac{Z_{0,x} + jZ_s\tan(\alpha)}{Z_s + jZ_{0,x}\tan(\alpha)}, Z_s\frac{Z_{0,y} + jZ_s\tan(\alpha)}{Z_s + jZ_{0,y}\tan(\alpha)}, Z_p\frac{Z_{0,z} + jZ_p\tan(\beta)}{Z_p + jZ_{0,z}\tan(\beta)}\right] \text{ with } \alpha = \sqrt{\frac{\rho}{\mu}}\omega d\,,\ \beta = \sqrt{\frac{\rho}{2\mu+\lambda}}\omega d\,, \quad (5)$$

with $Z_{0,x}, Z_{0,y}, Z_{0,z}$ denoting the diagonal elements of the boundary impedance $\tilde{\boldsymbol{Z}}_0$.

2.4. *Adaption to viscous and viscoelastic media*

The above formulas were derived for an elastic medium utilizing Lamé's constants μ and λ. To cover viscous liquids as well, equivalent elastic constants are determined for the fluid parameters. Liquids are described by the (nonlinear) Navier-Stokes equations, with two different Lamé's constants λ_f and μ_f (a.k.a dynamic viscosity η) and a coupling relation for pressure and density [8]. If the convective (nonlinear) part of the Navier-Stokes equations is neglected and time harmonic excitation is considered, the liquid parameters can be related to the equivalent elastic parameters $\mu \triangleq j\omega\eta$ and $\lambda \triangleq \rho_f c_0^2 + j\omega\lambda_f$ with ρ_f and c_0 denoting liquid mass density and speed of sound, respectively. Furthermore, the Stokes hypothesis $\lambda_f = -2\eta/3$ is applied [9]. Viscoelasticity can be implemented as superposition of elastic and viscous media.

3. Examples and conclusions

The described method is used to demonstrate the coupling between the spectral shear- and pressure impedances first for a water half-space, see Fig. 2, with $\rho = 1000\mathrm{kg/m^3}, \eta = 1\mathrm{mPa\,s}$, where only excitation in x direction is considered at a vibration frequency of 1.8MHz. Strong coupling occurs only at wavenumbers where the real part of l_p is small, resulting in one peak in Fig. 2 (left). In Fig. 3 impedances for a 1mm thick water layer with free surface, rigid backing and backing by a 0.5mm thick steel layer ($\rho = 7870\mathrm{kg/m^3}$, $Y = 210\mathrm{GPa}$, $\nu = 0.3$) are shown. An

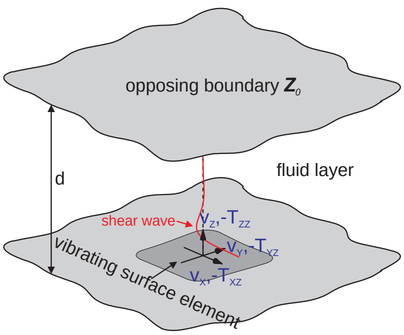

Figure 1: The liquid layer exerts shear- (T_{xz}, T_{yz}) and pressure stresses T_{zz} to the vibrating bottom surface excited by the prescribed surface velocities v_x,v_y and v_z.

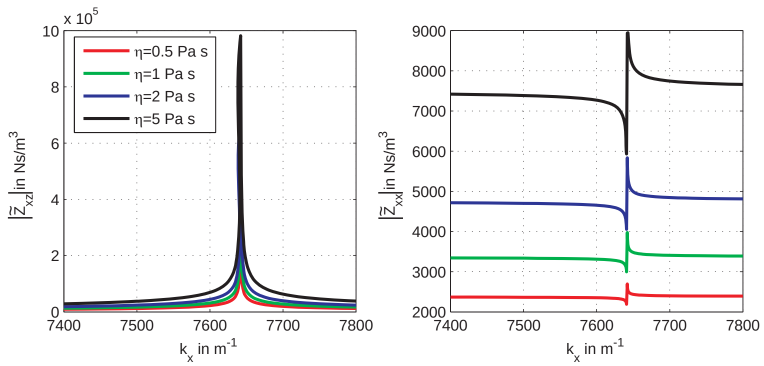

Figure 2: For the half-space ($d \to \infty$) coupling between shear- and pressure wave occurs (left) which also affects the apperent shear-impedance $\tilde{Z}_{xx}$ (right). The effect is shown for different viscosities.

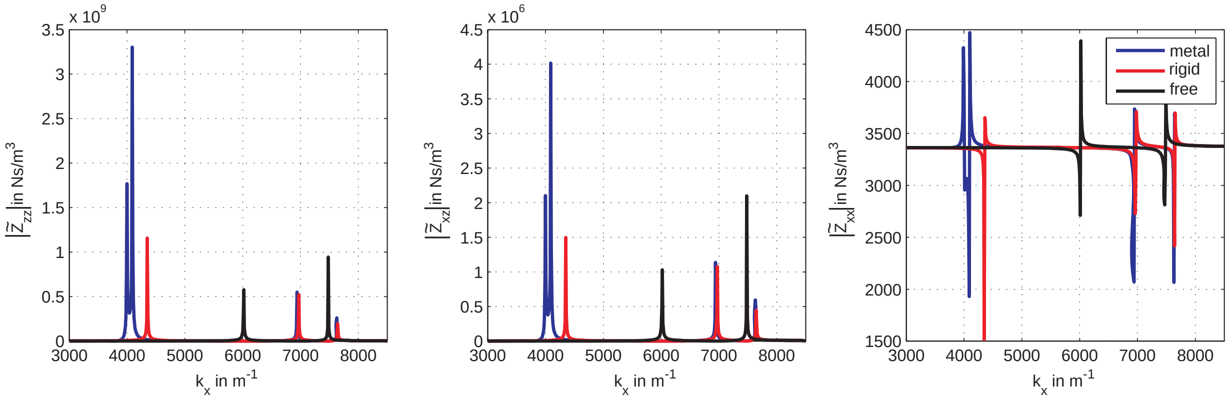

Figure 3: For a bounded layer (here 1mm water), multiple peaks emerge in the vicinity of wavenumbers where the pressure waves are stationary. The impedances are calculated for three different boundary conditions: 0.5mm thick metal layer, rigid boundary and free surface.

increase of the layer thickness d results in an increased number of peaks with lower amplitude, converging to the half-space results as d tends to infinity. The described method can be used to analyze loading effects of isotropic media. Furthermore, the given formulation can be used to calculate the fields within layered structures efficiently in the spectral domain. The method has been applied for viscous liquid layers to investigate effects of pressure and shear wave coupling.

4. Acknowledgment

This work is partly supported by the Austrian Center of Competence in Mechatronics (ACCM)

References

[1] K. Kanazawa, J. Gordon, Frequency of a quartz microbalance in contact with liquid, Anal. Chem. 57 (1985) 1770–1771.
[2] T. Voglhuber-Brunnmaier, E. K. Reichel, B. Jakoby, Characterization of a novel membrane-rheometer utilizing a semi-numerical modelling approach in the spectral domain, Sensors and Actuators A: Physical 162 (2) (2010) 310 – 315, eurosensors XXIII, 2009.
[3] R. Beigelbeck, B. Jakoby, A two-dimensional analysis of spurious compressional wave excitation by thickness-shear-mode resonators, Journal of Applied Physics 95 (9) (2004) 4989–4995.
[4] T. Lindenbauer, B. Jakoby, Fully three-dimensional analysis of tsm quartz sensors immersed in viscous liquids, in: Proc. IEEE Sensors, 2005, pp. 1249–1252.
[5] B. Jakoby, Efficient semi-numerical analysis of acoustic sensors using spectral domain methods a review, Meas. Sci. Technol. 19 (2008) 052001.
[6] H. H. E. Leipholz, U. Leipholz, Theory of Elasticity, Springer Verlag Gmbh, 1974.
[7] B. A. Auld, Acoustic Fields and Waves in Solids: Vol 1, John Wiley, New York, 1973.
[8] G. Batchelor, An Introduction to Fluid Dynamics, Cambridge University Press, 1967.
[9] H. Schichting, K. Gersten, Boundary Layer Theory, Springer Verlag Gmbh, 2003.

Appendix A. Matrix expressions

$$k_r^2 = k_x^2 + k_y^2 \quad , \; l_s = \sqrt{k_r^2 - \frac{\rho\omega^2}{\mu}} \; , \; l_p = \sqrt{k_r^2 - \frac{\rho\omega^2}{2\mu+\lambda}}$$

$$\boldsymbol{V}_{11} = \begin{bmatrix} -k_y^2 - l_s^2 & k_x k_y & -jk_x l_s \\ k_x k_y & -k_x^2 - l_s^2 & -jk_y l_s \\ jk_x l_s & jk_y l_s & -l_s l_p \end{bmatrix} \quad , \; \boldsymbol{V}_{12} = j\omega \begin{bmatrix} k_y^2 + l_s^2 & -k_x k_y & -jk_x l_s \\ -k_x k_y & k_x^2 + l_s^2 & -jk_y l_s \\ jk_x l_s & jk_y l_s & l_s l_p \end{bmatrix}$$

$$\boldsymbol{V}_{21} = \frac{\mu l_s}{j\omega} \begin{bmatrix} k_r^2 + l_s^2 & 0 & 2jk_x l_p \\ 0 & k_r^2 + l_s^2 & 2jk_y l_p \\ -2jk_x l_s & -2jk_y l_s & k_r^2 + l_s^2 \end{bmatrix} \quad , \; \boldsymbol{V}_{22} = \mu l_s \begin{bmatrix} k_r^2 + l_s^2 & 0 & -2jk_x l_p \\ 0 & k_r^2 + l_s^2 & -2jk_y l_p \\ 2jk_x l_s & 2jk_y l_s & k_r^2 + l_s^2 \end{bmatrix}$$